

# Evaluation of the CdS/CdTe heterojunction solar cell<sup>a)</sup>

Kim W. Mitchell,<sup>b)</sup> Alan L. Fahrenbruch, and Richard H. Bube

Department of Materials Science and Engineering, Stanford University, Stanford, California 94305  
(Received 14 December 1976; accepted for publication 27 May 1977)

A variety of CdS/CdTe heterojunction solar cells have been prepared by the vacuum evaporation of *n*-CdS films onto single-crystal *p*-CdTe substrates. Comparisons have been made between cells prepared using different substrate resistivities, substrate surface preparations, and CdS film resistivities. The mechanisms controlling the dark junction current, photocarrier collection, and photovoltaic properties with junction interface states present are modeled. A solar efficiency of 7.9% under 85 mW/cm<sup>2</sup> of solar simulator illumination was measured on a cell with an indium-tin-oxide coating and a glycerol antireflection coating.

PACS numbers: 84.60.Jt, 72.40.+w, 73.40.Lq

## I. INTRODUCTION

The CdS/CdTe heterojunction is a significant candidate for photovoltaic conversion of solar energy. Early investigations of CdS/CdTe heterojunctions focused on their applications as thin-film diodes and optical detectors,<sup>1-4</sup> while recent workers are exploring the potential of CdS/CdTe junctions for solar power generation.<sup>5-7</sup> Solar efficiencies in the past were typically 3–5%, with open-circuit voltages of 0.5–0.6 V, short-circuit current densities of 11–14 mA/cm<sup>2</sup>, and fill factors usually less than 50%. Recent reports by Yamaguchi *et al.*<sup>8</sup> and Nakayama *et al.*,<sup>9</sup> published since the completion of the work described in this paper, indicate that efficiencies greater than 10% have been achieved for film-on-crystal CdS/CdTe cells, and of 8% for all-thin-film CdS/CdTe cells. These authors, however, argue from their data that they really have *n*-CdS/*n*-CdTe/*p*-CdTe junctions, in which the CdS film is simply a contact to a CdTe homojunction; these were formed either by indiffusion of donors from the *n*-CdS into *p*-CdTe during junction formation<sup>8</sup> or by indiffusion of acceptors from *p*-Cu<sub>2</sub>Te used as an electrical contact to *n*-CdTe in the latter *n*-CdS/*n*-CdTe/*p*-CdTe/*p*-Cu<sub>2</sub>Te case.<sup>9</sup>

The purpose of this paper is to present data on relatively high efficiency CdS/CdTe heterojunction solar cells, to clarify some of the mechanisms that control the behavior of these cells, and to provide estimates of the future potential of CdS/CdTe solar cells.

## II. EXPERIMENTAL PROCEDURES

The solar cells were fabricated by vacuum deposition of *n*-CdS films on prepared *p*-CdTe single-crystal substrates. Two CdTe surface treatments were evaluated: (1) mechanical polishing with a final polish using 0.05  $\mu$ m alumina, and (2) a 1% bromine-in-methanol chemical polish following the mechanical polish. In addition, the effects of CdTe and CdS resistivity on the junction and photovoltaic properties were investigated using CdTe samples of 3 and 133  $\Omega$ cm resistivity and CdS films of about 1 and 0.005  $\Omega$ cm resistivity.

The substrates were prepared from *p*-CdTe single crystals<sup>10</sup> grown by the Bridgman method, doped with P

and excess Te. The CdS vacuum evaporation unit used a Varian model 3117 oil-diffusion-pumped vacuum system, which attains pressures in the 10<sup>-8</sup>-Torr range in the bell jar. During evaporation, a Meissner trap with circulating liquid N<sub>2</sub> enclosing the evaporation unit maintains the chamber pressure in the low 10<sup>-7</sup>-Torr range. The molecular beam sources are of the Knudsen-cell type, machined from solid high-purity Mo and resistance heated.

For the series of cells with 1- $\Omega$ cm CdS, powdered crystalline CdS was evaporated onto the substrates that were heated to 220°C. The resistivity of the CdS films was reduced to about 1  $\Omega$ cm by heat treatment in H<sub>2</sub> at 400°C for 15 min. To investigate the effect of a high-conductivity CdS film on the cell properties, cells with 0.005- $\Omega$ cm CdS layers were fabricated by coevaporation of indium during compound vacuum evaporation of CdS onto 350°C substrates.

Evaporated indium made low-resistance Ohmic contacts to the CdS. Either Au or Ni was used for making electrical contacts to the *p*-CdTe. The CdTe surfaces were prepared by first mechanically polishing to remove compensated surface layers, then chemically etching with a saturated K<sub>2</sub>Cr<sub>2</sub>O<sub>7</sub>:H<sub>2</sub>SO<sub>4</sub>:H<sub>2</sub>O solution for a total of 2 min. The samples were then immediately mounted in the vacuum system and the system pumped down to less than 10<sup>-6</sup> Torr. 99.999% Au was evaporated from a tungsten filament to form the contacts.

The indium-tin-oxide (ITO) used as a transparent electrode to the CdS on one of the cells was rf sputtered using a Perkin-Elmer Randex Model 3140 Sputtering System.<sup>11</sup> A high-density ITO target was sputtered for 90 min in an Ar pressure of 2 $\times$ 10<sup>-2</sup> Torr at a potential of 2.5 kV. The substrate temperature was maintained at 200°C to minimize cross diffusion in the solar cell. Measurements of the films on glass indicated a film thickness of 1.09  $\mu$ m and a sheet resistance of 14.7  $\Omega$ /square.<sup>13</sup>

## III. RESULTS

The electrical properties of *n*-CdS/*p*-CdTe cells, illustrating the effect of different CdTe surface treatments and resistivities, are presented in Table I. The methanol-bromine (MB) etched cells are significantly better than the mechanically polished cells. Their solar efficiency,  $V_{oc}$ ,  $J_{sc}$ , quantum efficiency, and fill factor

<sup>a)</sup>Work supported by NSF/RANN.

<sup>b)</sup>Present address: Sandia Laboratories, Division 5133, Albuquerque, N.M. 87115.

TABLE I. Photovoltaic properties of  $n$ -CdS/ $p$ -CdTe heterojunctions<sup>a</sup>. Illumination by solar simulator with 85 mW/cm<sup>2</sup>.

Property	3-Ω cm $p$ -CdTe MB <sup>a</sup> etch	133-Ω cm $p$ -CdTe MB <sup>a</sup> etch	3-Ω cm $p$ -CdTe Mech. polished	133-Ω cm $p$ -CdTe Mech. polished
$V_{oc}$ (V)	0.59	0.58	0.53	0.55
$J_{sc}$ (mA/cm <sup>2</sup> )	13.9	13.7	10.0	10.3
Quantum efficiency <sup>b</sup>	0.85	0.84	0.61	0.63
Fill factor	0.55	0.52	0.52	0.49
CdS resistivity (Ω cm) <sup>c</sup>	2.1	0.81	0.31	0.36
$J_0$ (A/cm <sup>2</sup> )	$2.8 \times 10^{-8}$	$10^{-9}$	$10^{-7}$	$8 \times 10^{-8}$
Diode factor $A$	1.80	1.48	2.02	2.07
Solar efficiency (%) <sup>d</sup>	5.2	4.9	3.3	3.2

<sup>a</sup>MB stands for methanol-bromine.

<sup>b</sup>Corrected for 17% reflection loss.

<sup>c</sup>Vacuum-evaporated CdS without In coevaporation; heat

treated in H<sub>2</sub> after deposition.

<sup>d</sup>Not corrected for 17% reflection loss.

for both mechanically polished and MB-etched cells, follows

$$J_0 = J_0 [\exp(qV/AkT) - 1], \quad (1)$$

with

$$J_0 = J_{00} \exp(-\Delta E/kT). \quad (2)$$

The dark values of  $J_0$  are lower for the MB-etched samples, on the order of  $10^{-8}$ – $10^{-9}$  A/cm<sup>2</sup>. The diode factors  $A$  are less than 2 for the MB-etched samples and approximately equal to 2 for the mechanically polished samples. Diode factors of 2 are indicative of recombination within the junction region; an ideal diffusion current would exhibit  $A=1$ . The variation of  $J_0$  with temperature for the 3-Ω cm CdTe cells is given in Fig. 1. In the higher-temperature region,  $\Delta E = 0.60$  eV and 0.59 eV for the mechanically polished and MB-etched cells, respectively. At temperatures below 294 °K, the relatively constant  $J_0$  (and the fact that the  $\ln J$ -vs- $1/T$  slope is independent of bias voltage) suggests tunneling-dominated currents.

The temperature dependences of the open-circuit voltage for the 3-Ω cm CdTe cells are similar with  $\Delta V_{oc}/\Delta T = -2 \times 10^{-3}$  V/°K and extrapolated intercepts at 0 °K of about 1.20 V, consistent with the values calculated from

$$V_{oc} = (Ak/q) \ln(I_{sc}/I_{00})T + V_b, \quad (3)$$

where  $V_b$  is the junction built-in voltage. The highest measured value of  $V_{oc}$  (at 80 °K) is slightly larger than 1.0 V.

The effect of coevaporation of indium with the CdS to produce 0.005-Ω cm CdS layers on the electrical properties of the CdS/CdTe cells is summarized in Table II. The solar efficiencies and fill factors are somewhat lower than the cells in Table I, primarily due to the larger values of  $J_0$  and  $A$  for these cells. These larger values of  $J_0$  may be caused by diffusion of indium into the CdTe substrate during CdS deposition, and/or by increased tunneling through the narrowed depletion layer in the higher-conductivity CdS. As with the previous series, the mechanically polished CdTe is inferior to the MB-etched CdTe surface.

A layer of indium-tin-oxide (ITO) was deposited as a transparent electrode to the CdS on the 3-Ω cm MB-etched CdTe cell in Table I to reduce its front-layer resistivity from 2.09 to  $6.2 \times 10^{-3}$  Ω cm. Significant improvement in the photovoltaic properties of the cell are made through use of the ITO and partial antireflection coatings, as summarized in Table III. The solar efficiency increased from 5.2 to 7.9% through increases in  $V_{oc}$ ,  $J_{sc}$ , and fill factor. The  $J$ - $V$  characteristics of the cell under 85 mW/cm<sup>2</sup> solar simulator illumination are shown in Fig. 2. The increases in  $J_{sc}$ ,  $V_{sc}$ , and fill

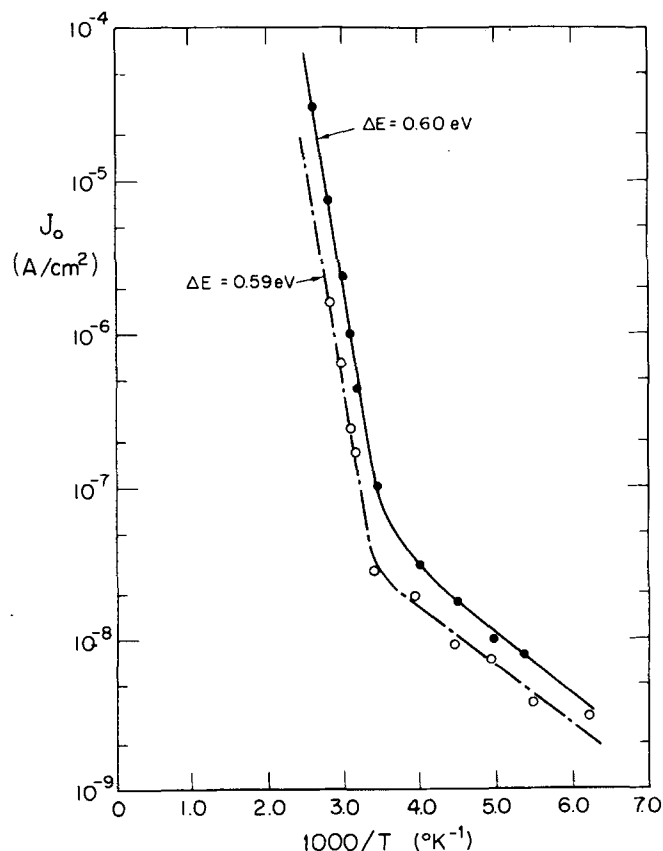


FIG. 1. Reverse saturation current  $J_0$  as a function of temperature for the 3-Ω cm CdTe samples: methanol-bromine etched (open circles), and mechanically polished (solid circles).

TABLE II. Photovoltaic properties of  $n$ -CdS/ $p$ -CdTe heterojunctions. Illumination by solar simulator with  $85 \text{ mW/cm}^2$ ; vacuum-evaporated CdS film with In coevaporation; resistivity on  $p$ -CdTe of  $0.0048 \Omega \text{ cm}$ .

Property	3- $\Omega \text{ cm}$ $p$ -CdTe MB <sup>a</sup> etch	133- $\Omega \text{ cm}$ $p$ -CdTe MB <sup>a</sup> etch
$V_{oc}$ (V)	0.62	0.52
$J_{sc}$ (mA/cm <sup>2</sup> )	11.7	14.6
Quantum efficiency <sup>b</sup>	0.72	0.89
Fill factor	0.54	0.48
$J_0$ (A/cm <sup>2</sup> )	$5 \times 10^{-7}$	$4.5 \times 10^{-6}$
Diode factor $A$	2.27	3.02
Solar efficiency (%) <sup>c</sup>	4.7	4.3

<sup>a</sup>MB stands for methanol-bromine.

<sup>b</sup>Corrected for 17% reflection loss.

<sup>c</sup>Not corrected for 17% reflection loss.

factor are consistent with the reduction of the reflection loss from 17 to about 6.5%, and a reduction of the series resistance. Theoretical calculations show that a fill factor that decreases with increasing  $I_L/I_0$  indicates series-resistance effects.<sup>14</sup> Before the ITO deposition, the fill factor decreased with increasing  $J_{sc}$  for  $J_{sc} > 2 \text{ mA/cm}^2$ ; with the ITO, the fill factor increased with increasing light intensity.

Since the above cell with ITO provided the most ideal behavior, additional measurements of the temperature dependence of the dark diode current, capacitance-voltage characteristics, minority-carrier diffusion lengths, spectral response, and the variation of the fill factor with light intensity were made. The dark diode current above  $294^\circ\text{K}$  followed Eqs. (1) and (2) with  $A = 1.89$ ,

TABLE III. Photovoltaic properties of cell E-11 3MB. The photovoltaic properties were measured under a solar simulator intensity of  $85 \text{ mW/cm}^2$ . The calculations are with respect to the active area of the cell and do not include the contact area.

	Initial <sup>a</sup>	ITO <sup>b</sup> 200°C, 90 min	Glycerol <sup>b</sup> AR coating
$V_{oc}$ (V)	0.59	0.62	0.63
$J_{sc}$ (mA/cm <sup>2</sup> )	13.9	14.4	16.1
Quantum efficiency (corrected for reflection)	0.80	0.79	0.82
Solar efficiency (%) (corrected for reflection)	6.3	7.5	8.4
(uncorrected)	5.2	6.5	7.9
Fill factor (%)	54.6	62.2	65.8
Reflection loss (%)	~17	~13	~6.5
Other Data			
$J_0$ (A/cm <sup>2</sup> ), 300°K	$2.8 \times 10^{-8}$	$2.0 \times 10^{-8}$	$1.7 \times 10^{-8}$
Diode factor $A$ , 300°K	1.80	1.89	1.89

<sup>a</sup>Total junction area =  $0.097 \text{ cm}^2$ ; active area =  $0.074 \text{ cm}^2$ .

<sup>b</sup>Total junction area =  $0.075 \text{ cm}^2$ ; active area =  $0.053 \text{ cm}^2$ .

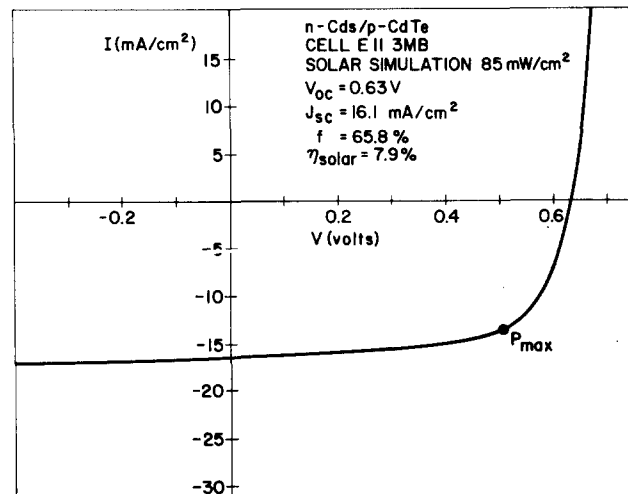


FIG. 2. Photovoltaic response of  $n$ -CdS/ $p$ -CdTe cell E-11 3MB.

$J_{00} = 350 \text{ A/cm}^2$ , and  $\Delta E = 0.59 \text{ eV}$ . Below  $294^\circ\text{K}$ , the dark current follows

$$J = J_{00} \exp(\beta T) \exp(\alpha V), \quad (4)$$

with  $\alpha = 21.9 \text{ V}^{-1}$ ,  $\beta = 0.015^\circ\text{K}^{-1}$ , and  $J_{00} = 2.4 \times 10^{-10} \text{ A/cm}^2$ .

The calculated depletion layer width for this cell from capacitance-voltage characteristics is  $0.19 \mu\text{m}$  at zero bias and  $0.29 \mu\text{m}$  at  $-1 \text{ V}$  bias. Since  $N_D \sim 6 \times 10^{18} \text{ cm}^{-3}$

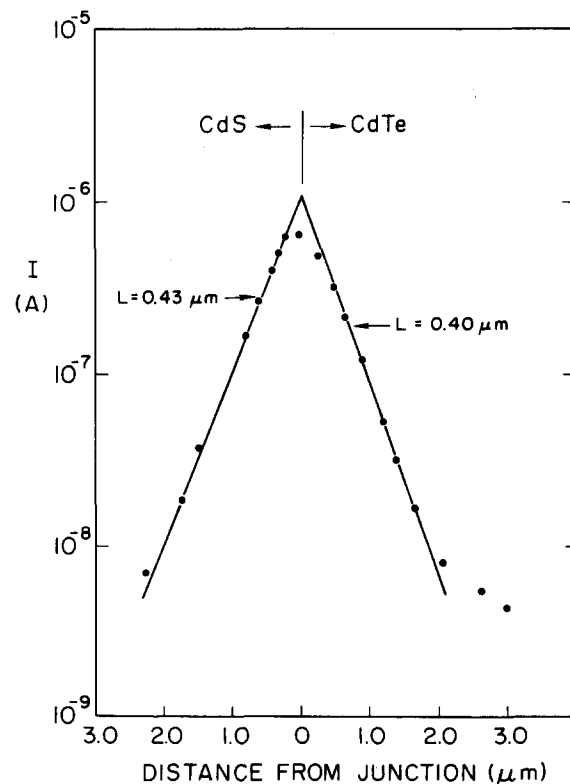


FIG. 3. Electron-beam-induced current as a function of beam position for cell E-11 3MB. The calculated values of the minority carrier diffusion lengths are  $0.40 \mu\text{m}$  in  $p$ -CdTe, and  $0.43 \mu\text{m}$  for  $n$ -CdS.

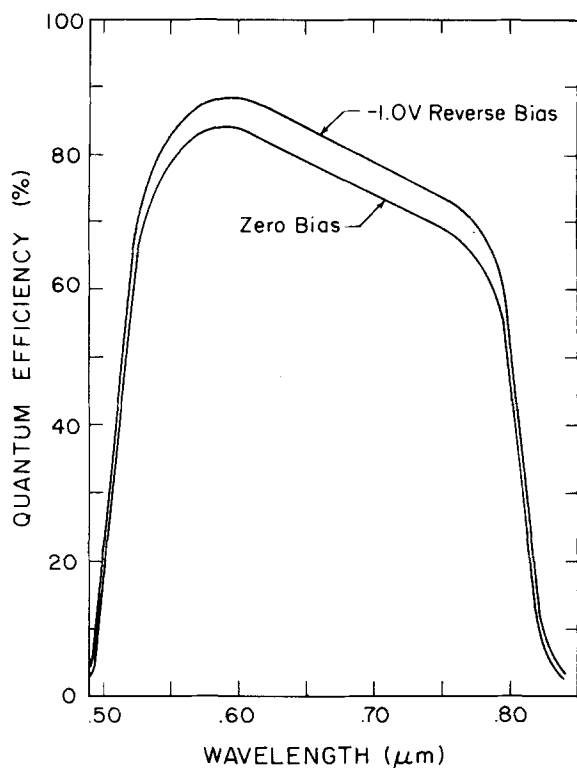


FIG. 4. Spectral response for cell E-11 3MB (corrected for 13% reflection loss) at zero and  $-1$  V bias.

$\gg N_A \sim 3.2 \times 10^{16} \text{ cm}^{-3}$ , the depletion layer is almost entirely in the CdTe.

Figure 3 is a plot of the electron-beam-induced current for a cleaved cross section of the  $3\text{-}\Omega\text{ cm}$  CdTe cell. The slope of the induced current versus beam position gives an effective diffusion length of  $0.40 \text{ }\mu\text{m}$  for the P-doped CdTe, and  $0.43 \text{ }\mu\text{m}$  for the CdS. The CdS value is in good agreement with Oakes and Greenfield's data for similar CdS films.<sup>15</sup> A bulk carrier lifetime of  $6 \times 10^{-11} \text{ sec}$  for the CdTe calculated from the diffusion length is qualitatively consistent with the high density of electrically inactive P present, if these act as recombination centers.<sup>16</sup>

The spectral response of the  $3\text{-}\Omega\text{ cm}$  CdTe cell is shown in Fig. 4 as a function of applied bias, corrected for a 13% reflection loss. The quantum efficiency represents the fraction of photons at each wavelength entering the cell that contribute to the light current. The quantum efficiency increases with reverse bias. For  $-1$  V bias, the maximum quantum efficiency is 0.89 at  $0.60 \text{ }\mu\text{m}$ . The ratio of the quantum efficiency at  $-1$  V bias to that at zero bias is a constant value of 1.06, independent of wavelength from  $0.52$  to  $0.80 \text{ }\mu\text{m}$ . The short-wavelength edge of the spectral response is defined by the optical transmission edge of the front layer consisting of the CdS and ITO. The shape of the long-wavelength edge is defined by the collection of photocarriers from the CdTe. New optical absorption data for CdTe have been calculated from the shape of this spectral response curve.<sup>17</sup>

The variation of the fill factor with the ratio  $I_L/I_0$  after the ITO deposition is shown in Fig. 5. Theoretical

calculations<sup>14</sup> of the fill factor, also shown in Fig. 5, indicate a divergence of the fill factor from ideality due primarily to the voltage dependence of the light current, represented by the collection function  $H(V)$ . The formulation of this collection function and its effect on the fill factor are described in Sec. IV.

#### IV. DISCUSSION

Models for the dark- and light-current mechanisms and an evaluation of the photovoltaic performance of the CdS/CdTe heterojunction can be developed on the basis of the previous data.

The diode behavior of the  $3\text{-}\Omega\text{ cm}$  MB-etched CdTe cell with ITO is consistent with the dark current being controlled by recombination at temperatures above  $294^\circ\text{K}$  and by tunneling at lower temperatures. The recombination current follows the form given by Eqs. (1) and (2).<sup>18,19</sup> The theoretical junction built-in voltage  $V_b = 1.18 \text{ V}$ , in agreement with the value calculated from the product  $A\Delta E$ . The difference between the measured value of 1.89 for the diode factor and the ideal value of 2.0 is due to the voltage dependence of  $J_{00}$ .<sup>18</sup> The midgap states that act as recombination centers may arise either from states already present in the CdTe or from states created as a result of junction fabrication or the lattice mismatch between CdS and CdTe.

The dark current behavior below  $294^\circ\text{K}$  is consistent with tunneling, where the empirical temperature coefficient  $\beta$  for tunneling of 0.015 agrees closely with the value of 0.014 calculated from theory.<sup>18</sup> The acceptor concentration of  $3.2 \times 10^{16} \text{ cm}^{-3}$  in the CdTe is too low to allow simple one-step quantum-mechanical tunneling through the energy barrier at the junction. Applying the multistep tunneling-recombination model of Riben and Feucht,<sup>20,21</sup> the number of tunneling steps is calculated to be about 30, in agreement with the results of Adirovich *et al.*<sup>3</sup> for their CdS/CdTe heterojunctions.

The lower value of  $J_0$  for the methanol-bromine MB-etched CdTe surface compared to the mechanically

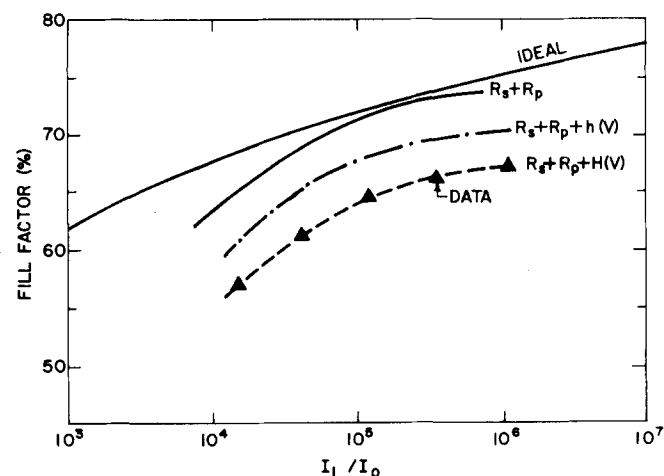


FIG. 5. The measured and calculated values of fill factor as a function of  $I_L/I_0$  for cell E-11 3MB with  $R_s = 5 \text{ }\Omega$ ,  $R_p = 2.7 \times 10^5 \text{ }\Omega$ ,  $I_0 = 1.3 \times 10^{-9} \text{ A}$ ,  $A = 1.89$ ,  $T = 300^\circ\text{K}$ ,  $h(V)$  the interface collection function, and  $H(V)$  the total collection function for the light current.

polished surface indicates that mechanically induced defects close to the interface act as recombination and tunneling centers, and that the MB etch significantly reduces their concentration.

The light current in the cell is determined by the number of available photons and the quantum efficiency of the cell. For a solar intensity of  $85 \text{ mW/cm}^2$  at AM2, the photon flux within the bandpass window ( $0.52\text{--}0.84 \mu\text{m}$ ) for the CdS/CdTe cell is equivalent to a current density of  $21.1 \text{ mA/cm}^2$ .<sup>18,22</sup> The quantum efficiency is determined by the absorption of photons and the subsequent collection of photogenerated minority carriers. Losses in the collection of photocarriers can occur either in the bulk or at the junction interface. If it is assumed that all carriers generated within a depletion-layer width  $W$  of the interface are collected without loss, and that all carriers generated at a distance greater than  $W$  from the interface are collected with an attenuation factor of  $\exp[-(x-W)/L]$ , where  $L$  is the bulk minority-carrier diffusion length, then<sup>18,23</sup>

$$g(V) = 1 - (1 + \alpha L)^{-1} \exp(-\alpha W), \quad (5)$$

where  $\alpha$  is the optical absorption coefficient. The collection of photocarriers through the junction interface can be approximated by<sup>18,24</sup>

$$h(V) = (1 + S/\mu E_0)^{-1}, \quad (6)$$

where  $S$  is the interface recombination velocity,  $\mu$  is the electron mobility within the junction region, and  $E_0$  is the electric field at the junction. The quantum efficiency corrected for reflection loss is then

$$Q(\lambda) = H(V) = h(V)g(V), \quad (7)$$

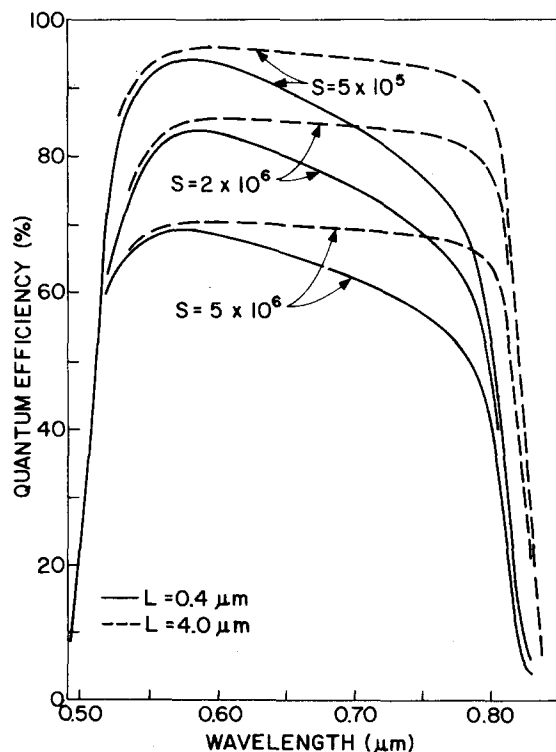


FIG. 6. Theoretical spectral response curves for an  $n\text{-CdS}/p\text{-CdTe}$  cell with  $N_A = 3.2 \times 10^{16} \text{ cm}^{-3}$  for different values of interface recombination velocity  $S$ , in  $\text{cm/sec}$ , and minority-carrier diffusion length  $L$ .

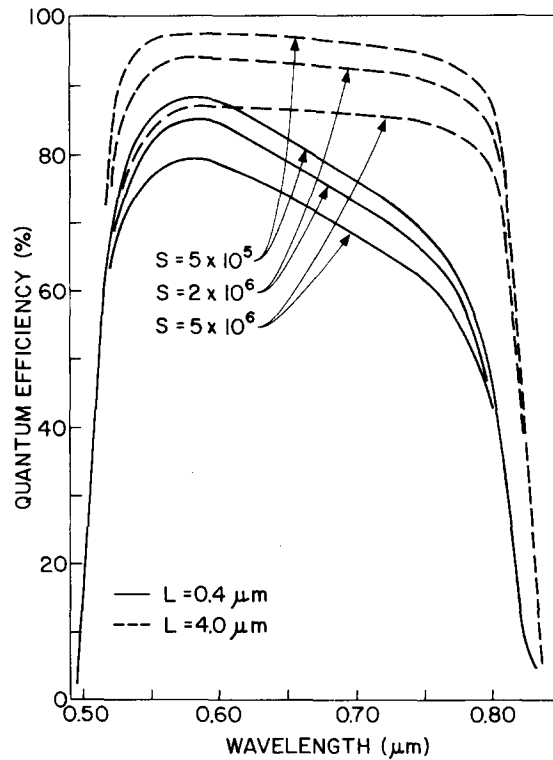


FIG. 7. Theoretical spectral response curves for an  $n\text{-CdS}/p\text{-CdTe}$  cell with  $N_A = 3.2 \times 10^{17} \text{ cm}^{-3}$  for different values of interface recombination velocity  $S$ , in  $\text{cm/sec}$ , and minority-carrier diffusion length  $L$ .

assuming that each absorbed photon produces an electron-hole pair. From the spectral response curve at short wavelengths [where  $g(V) \sim 1$ ], values of  $h(V) = 0.84$  at zero bias and  $h(V) = 0.89$  at  $-1 \text{ V}$  bias are derived for the  $3\text{-}\Omega\text{cm}$  MB-etched CdTe cell. From Eq. (6), the interface recombination velocity for this cell is calculated to be about  $2 \times 10^6 \text{ cm/sec}$ .

A comparison of the average values of quantum efficiency listed in Tables I and II show that the cells prepared on mechanically polished CdTe have significantly lower quantum efficiencies than those cells prepared on MB-etched surfaces. Thus the MB etch not only reduces  $J_0$  but also improves the quantum efficiency.

Significant improvements in the light current of the  $n\text{-CdS}/p\text{-CdTe}$  solar cell can be made by increasing both the minority-carrier diffusion length and/or the effective acceptor doping in the CdTe. Figures 6 and 7 illustrate the variations in the theoretical response of the quantum efficiency for acceptor concentrations of  $3.2 \times 10^{16} \text{ cm}^{-3}$ , as used here, and  $3.2 \times 10^{17} \text{ cm}^{-3}$ ; for diffusion lengths of  $0.40 \mu\text{m}$ , as used here, and  $4.0 \mu\text{m}$ ; for values of the interface recombination velocity of  $5 \times 10^5 \text{ cm/sec}$ ,  $2 \times 10^6 \text{ cm/sec}$ , as used here, and  $5 \times 10^6 \text{ cm/sec}$ . Increasing the acceptor concentration to  $3 \times 10^{17} \text{ cm}^{-3}$  is feasible, as reported by Gu *et al.*<sup>25</sup> and Adirovich *et al.*<sup>3</sup> Polycrystalline thin-film CdTe is expected to give comparable or better quantum efficiencies, as was demonstrated by Fahrenbruch *et al.*<sup>6</sup> who obtained a quantum efficiency of 85% in a cell made by close-spaced vapor transport of CdTe onto single-crystal CdS.

TABLE IV. Comparison of theoretical and measured photovoltaic properties of cell E-11 3MB.

	Ideal junction calculation <sup>a</sup>	Measured values <sup>b</sup>
$J_0$ (A/cm <sup>2</sup> )	$3.2 \times 10^{-10}$	$1.7 \times 10^{-8}$
Diode factor $A$	2.0	1.89
$J_{sc}$ (mA/cm <sup>2</sup> )	21.1	16.1
$V_{oc}$ (V)	0.90	0.63
$V_m$ (V)	0.76	0.51
$J_m$ (mA/cm <sup>2</sup> )	19.8	13.3
Fill factor	0.79	0.66
Quantum efficiency	1.0	0.82
Solar efficiency (%)	17.6	7.9

<sup>a</sup>Calculated for solar illumination of 85 mW/cm<sup>2</sup> assuming recombination-dominated  $J_0$  with  $\tau = 6 \times 10^{-11}$  sec and neglecting any losses from series resistance, shunt resistance, reflection, less-than-unity quantum efficiency, or less-than-unity area ratio because of electrodes.

<sup>b</sup>Measured values under 85 mW/cm<sup>2</sup> of solar simulator illumination for the cell with an indium-tin-oxide coating, and a glycerol antireflection coating, with an optical reflection loss of 6.5%. The calculations are with respect to the active area of the cell and do not include the contact area; total area = 0.075 cm<sup>2</sup>, active area = 0.053 cm<sup>2</sup>.

Table IV compares the solar-cell parameters for a  $n$ -CdS/ $p$ -CdTe heterojunction as calculated theoretically for an ideal junction and as achieved to date in the work of this paper. The various contributions to the lower efficiency of the real cell are summarized in Table V to pinpoint the areas where improvement is necessary. The collection function  $H(V)$  strongly influences the efficiency; if  $H(V) = 1.0$ , then  $J_{sc} = 19.7$  mA/cm<sup>2</sup>,  $V_{oc} = 0.66$  V,  $f = 0.75$ , and the solar efficiency would be 11.5%. Alternatively, if  $J_0$  were reduced by a factor of 50 by treatment of the interface, for the same  $H(V)$  observed above,  $V = 0.83$  V,  $f = 0.70$ , and the solar efficiency would be 11.1%.

## V. CONCLUSIONS

A solar efficiency of 7.9% has been measured under 85 mW/cm<sup>2</sup> solar simulator illumination on a  $n$ -CdS/ $p$ -CdTe cell with an indium-tin-oxide coating and a glycerol antireflection coating. This measured efficiency is lower than the ideal efficiency of 17.6% for this heterojunction primarily because of the larger value of  $J_0$  and a voltage dependence in the collection of photocar-

riers, defined as the collection function  $H(V)$ . The collection function not only reduces the quantum efficiency to 0.82, but also significantly reduces the fill factor.

For the  $n$ -CdS/ $p$ -CdTe solar cell,  $H(V)$  can be expressed as the product of a bulk collection term  $g(V)$ , representing the fraction of photocarriers arriving at the junction, and an interface collection term  $h(V)$ , representing the fraction of photocarriers safely passing through the junction upon reaching it. Although the minority-carrier diffusion length in the bulk CdTe used in this investigation is only 0.40  $\mu$ m, the collection of photocarriers from the bulk is still high due to the large optical absorption coefficients of CdTe. At the acceptor concentration used of  $3.2 \times 10^{16}$  cm<sup>-3</sup> in the 3- $\Omega$  cm CdTe, the interface collection function  $h(V)$  is strongly dependent on the interface recombination velocity  $S$ , as shown in Fig. 6. The value 0.84 for  $h(0)$  implies an interface recombination velocity of  $2 \times 10^6$  cm/sec.

Future improvements in the solar efficiency of CdS/CdTe heterojunctions will come primarily through improved fabrication techniques and materials. CdTe with minority-carrier lifetimes greater than  $6 \times 10^{-11}$  sec would increase the efficiency through longer diffusion lengths, improving photocarrier collection, and lower values of  $J_0$ , giving larger open-circuit voltages and fill factors. Increasing the effective CdTe acceptor concentration to  $10^{17}$  cm<sup>-3</sup> would be significant in minimizing the effects of the interface recombination velocity  $S$ , as shown in Fig. 7. CdS/CdTe heterojunction solar cells with solar efficiencies of 10–15% are possible with higher-quality CdTe, through improved photocarrier collection, and with lower values of  $J_0$ .

TABLE V. Summary of losses in  $n$ -CdS/ $p$ -CdTe solar cell compared to theoretical ideal.

Loss in $J_{sc}$	Loss in $V_{oc}$	Loss in $f$
6.5% reflection loss		
$Q = 0.82$	Larger $J_0$	Smaller $I_{sc}/I_0$
Small $L = 0.4$ $\mu$ m	Smaller $J_{sc}$	$R_s = 5$ $\Omega$
Large $S = 2 \times 10^6$ cm/sec	Smaller $A$	$R_p = 2.7 \times 10^5$ $\Omega$
	29% area loss due to contacts	$H(V) = 0.90$

<sup>1</sup>R.S. Muller and R. Zuleeg, J. Appl. Phys. 35, 1550 (1964).

<sup>2</sup>R.W. Dutton and R.S. Muller, Solid-State Electron. 11, 749 (1968).

<sup>3</sup>E.I. Adirovich, Y.M. Yuabov, and G.R. Yagudaev, Sov. Phys.-Dokl. 15, 553 (1970); Phys. Status Solidi A 6, 311 (1971); *Proceedings, International Conference on the Physics and Chemistry of Semiconductor Heterojunctions*, edited by G. Szigeti (Akademiai Kiado, Budapest, 1971) Vol. 2, p. 151.

<sup>4</sup>D. Bonnet and H. Rabenhorst, *Proceedings International Conference on the Physics and Chemistry of Semiconductor Heterojunctions*, edited by G. Szigeti (Akademiai Kiado, Budapest, 1971), Vol. 1, p. 119.

<sup>5</sup>D. Bonnet and H. Rabenhorst, *Proceedings, 9th IEEE Photovoltaic Spec. Conf.* (IEEE, New York, 1972), p. 129.

<sup>6</sup>A. Fahrenbruch, V. Vasilchenko, F. Buch, K. Mitchell, and R.H. Bube, Appl. Phys. Lett. 25, 605 (1974).

<sup>7</sup>K. Yamaguchi, N. Nakayama, H. Matsumoto, Y. Hioki, and S. Ikegami, Jpn. J. Appl. Phys. 14, 1397 (1975).

<sup>8</sup>K. Yamaguchi, H. Matsumoto, N. Nakayama, and S. Ikegami, Jpn. J. Appl. Phys. 15, 1575 (1976).

<sup>9</sup>N. Nakayama, H. Matsumoto, K. Yamaguchi, S. Ikegami, and Y. Hioki, Jpn. J. Appl. Phys. 15, 2281 (1976).

<sup>10</sup>Crystals grown by R. Raymakers of the Crystal Growth Laboratory of the Center for Materials Research at Stanford University.

<sup>11</sup>Sputtering done by W. Holmes in the Vapor Deposition Laboratory of the Center for Materials Research at Stanford University.

<sup>12</sup>Target obtained from Haselden Co., San Jose, Calif.

<sup>13</sup>High-optical-quality ITO films with sheet resistances of 5 to 15  $\Omega$ /square with corresponding resistivities of  $2.0 \times 10^{-4}$  to  $1.6 \times 10^{-3}$   $\Omega$  cm, have been made by this technique.

- <sup>14</sup>K.W. Mitchell, A.L. Fahrenbruch, and R.H. Bube, *Solid-State-Electron.* **20**, 559 (1977).
- <sup>15</sup>J.J. Oakes and I.G. Greenfield, Report No. NSF/RANN/AER 72-03478 A04/TR 75/5, 1975 (unpublished).
- <sup>16</sup>The 3- $\Omega$  cm CdTe is doped with about  $10^{19}$  cm<sup>-3</sup> phosphorus impurities and 0.05% excess Te (the calculated electrical activity of the phosphorus impurity is 0.04%).
- <sup>17</sup>K.W. Mitchell, A.L. Fahrenbruch, and R.H. Bube, *J. Appl. Phys.* **48**, 829 (1977).
- <sup>18</sup>K.W. Mitchell, Ph.D. thesis (Stanford University, Stanford, Calif., 1976) (unpublished).
- <sup>19</sup>B.L. Harma and R.K. Purhoit, *Semiconductor Heterojunctions* (Pergamon, New York, 1974).
- <sup>20</sup>A.R. Riben and D.L. Feucht, *Solid-State Electron.* **9**, 1055 (1966).
- <sup>21</sup>A.R. Riben and D.L. Feucht, *Int. J. Electron.* **20**, 583 (1966).
- <sup>22</sup>The CdS film is sufficiently thick that no light absorbed in the CdS contributes to the light current.
- <sup>23</sup>J.P. Donnelly and A.G. Milnes, *Int. J. Electron.* **4**, 295 (1966).
- <sup>24</sup>K.W. Boer and J.D. Meakin, Report No. NSF/RANN/AER 72-03478 A03/FR/75, 1975 (unpublished).
- <sup>25</sup>J. Gu, T. Kitahara, S. Fujita, and T. Sakaguchi, *Jpn. J. Appl. Phys.* **14**, 499 (1975).